Comparison of the Transient Behaviors of Bubbling and Circulating Fluidized Bed Combustors

Guillermo Martinez Castilla, Rubén. M. Montañés, David Pallarès & Filip Johnsson

Published online: 04 Apr 2022.

Submit your article to this journal ↗

View related articles ↗

View Crossmark data ↗

Taylor & Francis
Taylor & Francis Group

OPEN ACCESS

Check for updates

Comparison of the Transient Behaviors of Bubbling and Circulating Fluidized Bed Combustors

Guillermo Martinez Castilla[a], Rubén. M. Montañés[b], David Pallarès[a], and Filip Johnsson[a]

[a]Division of Energy Technology, Department of Space, Earth and Environment, Chalmers University of Technology, Gothenburg, Sweden; [b]SINTEF Energy Research, Trondheim, Norway

ABSTRACT

This work compares the transient behaviors of the flue gas sides of large-scale bubbling and circulating fluidized bed (BFB and CFB, respectively) boilers. For this purpose, a dynamic model of the in-furnace side of fluidized bed combustors presented and validated by the authors in a former work is used to simulate two industrial units. The results show that for load changes the heat transfer to the waterwalls stabilizes more rapidly in BFB units. Differences in stabilization time between the dense bed and the top of the furnace are observed in both units, caused by the distribution of solids along the combustor: the dense bed contains more solids than regions located higher up in the furnace and, therefore slower to respond, with stabilization times of around 15 minutes, as compared to stabilization times in the range of 1–8 minutes for the upper furnace. This behavior is accentuated in the BFB, where all the solids remain in the dense bottom region. The effect of the characteristic times of the main in-furnace mechanisms (fluid-dynamics, fuel conversion, and heat transfer) on the dynamic performance of BFB and CFB units has been explored and expressed through proposed mathematical relationships.

Introduction

Fluidized bed combustion (FBC) has become a preferred choice for the thermal treatment of solid fuels since the 1970s and 1980s. Thanks to the unique, inherent strong mixing and heat transfer capabilities of the fluidized bed (FB) units, fuels of very different natures can be thermally converted in these boilers. These fuels range from different types of biomass to coal and municipal solid waste, as well as mixtures thereof. This allows FBC facilities to switch fuels and to co-fire fuel mixtures depending on fuel price and availability. Furthermore, fluidized bed combustors achieve relatively low levels of emissions through cost-efficient, in-bed capture and reduction methods and high combustion and generation efficiencies, what makes them crucial components in many energy systems worldwide.

Depending on the fluidization velocity, fluidized bed combustors can be divided into bubbling and circulating fluidized beds (BFB and CFB, respectively). CFB units operate under conditions in which a significant amount of solids is entrained by the gas, being

externally recirculated into the riser through a cyclone and a loop seal that prevents the gas entering the cyclone from its leg. In contrast, BFB boilers are operated at lower fluidization velocities, so the amount of solids carried by the gas flow is not significant. These conceptual differences related to both the design and operation of FB boilers result in very different behaviors, which need to be understood for the optimal design and operation of the boilers. In particular, there are substantial differences regarding the heat transfer to the steam cycle. BFB risers have very low concentrations of solids in most parts of the furnace, with radiation being the main phenomenon governing heat transfer to the waterwalls. In contrast, a large flow of solids down by the walls makes convection the governing mechanism in CFB units [1]. Little has been published comparing the operating performances of BFB and CFB boilers. One of the most detailed reviews on this topic published to date is that of Koornneef et al. [2], who showed the commercial size limitation of BFB boilers. Thus, BFB boilers are mostly used for fuels

Nomenclature

A	area, m^2	**Subscripts**	
BFB	bubbling fluidized bed	c	core
c	concentration, kg m^{-3}	char	related to char conversion
C_p	heat capacity at constant pressure, J kg^{-1} K^{-1}	cyclone	in the cyclone
CFB	circulating fluidized bed	db	dense bed
F	view factor, mass flow, kg s^{-1}	FC	fuel conversion
FB	fluidized bed	FD	fluid dynamics
FBC	fluidized bed combustion/combustor	g	gas, gas volume
h	convective heat transfer coefficient, W m^{-2} K^{-1}	HT	heat transfer
HHV	high heating value, MJ kg^{-1}	i	region, element
k	absorption coefficient, m^{-1}	in	entering the surface
L	length, m	j	other surfaces
m	mass, kg	k	other cells
q	heat flux in a certain surface/region/volume, W	loop-seal	in the loop seal
q″	heat flux per unit area, W m^{-2}	net	net absorbed radiation
Q	total heat flux, W	rad	radiation
RC	relative change, %	riser	in the riser
t	time, s	s	stabilization
T	temperature, °C	side	from core to wall layer
y	value of a certain variable y	surf	surface
		top	top of the riser
		vol	volume
Greek symbols		w	wall
α	absorptivity	wl	wall layer
ε	voidage, emissivity	0	before the change is introduced
σ	Stefan-Boltzmann constant [5.6 · 10^{-8} W m^{-2} K^{-4}]	∞	after new steady state is reached
η	efficiency		
τ	characteristic time, s		

that have a lower energy density, i.e., are associated with higher energy transport costs, such as biomass, whereas CFB boilers can be applied in a cost-efficient way at utility scales. DeFusco et al. [3] presented a case study assessing the operability and financial differences of BFB and CFB boilers for 50-MW biomass combustion. In that study, it was suggested that a BFB unit would be more beneficial due to its lower capital and operational costs, as well as its greater fuel flexibility. It was also stated that CFB units are the preferred option when fresh biomass is co-fired with fuels of higher heating value (including low-moisture fuels, such as urban waste wood).

Given that fuel conditions are highly variable (e.g., with respect to the fuel mixture, moisture content and heating value), it is crucial to understand the transient operation of FBC units in order to design satisfactory control systems to keep the temperature field and heat transfer within operability limits. In addition, when commissioned in energy systems that are progressively increasing their penetration levels of non-dispatchable generation of heat and power, fluidized bed boilers will be required to operate in cycling mode, thereby emphasizing the need for fast and controlled load ramping and startup and shut-down capabilities.

Over the last decade, dynamic modeling and simulation have gained extensive recognition as an effective

tool for assessing the dynamic behavior and capabilities of thermal power plants, among others [4–7]. The main purpose of dynamic models is to track key process variables over time, so as to predict their behaviors when a certain event or transition occurs. Furthermore, dynamic models are used to test different control strategies and to train operators. When it comes to combustion plants, dynamic modeling of the flue gas side of the boiler provides insights into the combustion process under varying operational conditions. In addition, dynamic models of the flue gas side can be integrated into dynamic process models of the steam cycle, thereby allowing the study of the dynamic interactions between the two systems under transient operation.

Mathematical modeling of FBC units has been covered by several researchers in the past few decades. However, the main focus has been on steady or quasi-steady state models (for semi-empirical and CFD modeling, respectively), which provide useful knowledge for the design and operation of FBC units around a given operating condition. Considerably less work has been carried out in the area of dynamic modeling of FB boilers. Regarding CFB combustors, some authors have focused on the combustion dynamics [8], targeting estimations of the residence time of solids and the char inventory over time. Several 0D dynamic models have been published (see

[9–11]), despite the fact they are not capable of predicting the spatial distribution of solids throughout the furnace, a critical aspect of CFB operation. As one of the first 1D dynamic models, Park and Basu [12] aimed to predict the concentrations of char and oxygen after a fuel shift, presenting a model that was validated against a 0.3-MW unit. Chen and Xiaolong [13] published a dynamic model of a 410 t/h coal CFB unit, which was applied to resemble a specific dynamic operation of the target boiler. More recently, Kim et al. [14] published a 1.5D model validated with design data from a coal-fired 795-MW plant. Their subsequent study revealed overshoots in the freeboard temperatures for certain load changes. Stefanitsis et al. [15] have utilized a dynamic model of a CFB combustor built in APROS to evaluate the transient performance of a CFB boiler after the addition of a thermal energy storage in the form of hot bulk solids in an external BFB, concluding that the stabilization times of the boiler were reduced after the removal of solids for storage. Other groups have focused their efforts on developing dynamic models to design and test control structures (see [16, 17]). When it comes to BFB units, published work is even scarcer. Kataja and Majanne [18] presented a dynamic model of a coal-fired BFB boiler that included both the flue gas side and steam-water side, and applied it to simulate changes in the fuel feed and fuel moisture content. A similar model was presented by Selcuk and Degirmenci [19], which was validated against a 0.3-MW pilot plant. Galgano et al. [20] developed a model of a biomass-fired BFB unit, uncovering large differences between the transient responses of the dense bed and the freeboard caused by the differences in heat capacities. Surasani et al. [21] published a dynamic representation of BFB combustors, which was validated with steady-state data from a laboratory-scale unit. The authors concluded that a description of the changes in fuel properties throughout conversion was required for more accurate predictions of the dynamics.

In summary, there is a lack of knowledge regarding the dynamics of the flue gas side of fluidized bed boilers in transient operation, especially regarding the role played by the different governing mechanisms, and the differences between bubbling and circulating units in their abilities to meet future demand sides characterized by stronger and faster fluctuations due to the increased presence of variable renewable energy generation. More specifically, there is a lack of works that use models validated against operational data from large-scale plants.

This work aims at identifying and quantifying the mechanisms governing the dynamics of large-scale fluidized bed boilers and comparing the response on the flue gas side of BFB and CFB boilers of the same size in defined transient scenarios. For this, we use a dynamic model of the flue gas side of FB combustors, that was previously validated against industrial operational data and that is capable of describing both BFB and CFB units, to simulate two industrial-scale furnaces of the same size (130 MW$_{th}$). The inherent transient responses of the system when load and fuel moisture content change are computed. Furthermore, the present work analyses the dependence of the stabilization times of the flue-gas side of BFB and CFB combustors on the characteristic times of the main in-furnace mechanisms (i.e., fluid dynamics, fuel conversion and heat transfer).

Model description

This work makes use of the model presented by the authors in a previous publication [22], which provides a comprehensive description and validation of the model. Note that for the model validation presented in [22], steady-state and transient operational datasets of the units in which the present study is based on were used. Results of the validation showed deviations between the simulated and measured values of less than 10% for all operating conditions, with a mean error of 1.9% for calibration cases and of 4.7% for validation cases. Hence, it can be stated that based on the results shown in [22], the model is successfully validated for the purpose of this work. The present section summarizes the main characteristic of the model, paying special attention to the main differences that arise when modeling the dynamic behaviors of BFB and CFB units.

The model is built in Modelica [23] and run in the environment Dymola [24]. The selection of such language and software is due to the fact that the model is built to be integrated into multi-domain transient plant models of the water-steam side, for which Modelica is, to the judgment of the authors, the most suitable alternative. The model consists of an assembly of control volumes that exchange mass and energy. The model covers the entire range of operations of FB combustors, i.e., it is capable of simulating both bubbling and circulating conditions (BFB and CFB) as presented in the subsections below, over the load ranges typically covered by the technology. This is achieved by i) distinguishing between CFB and a BFB mode in the model and setting for each of them a
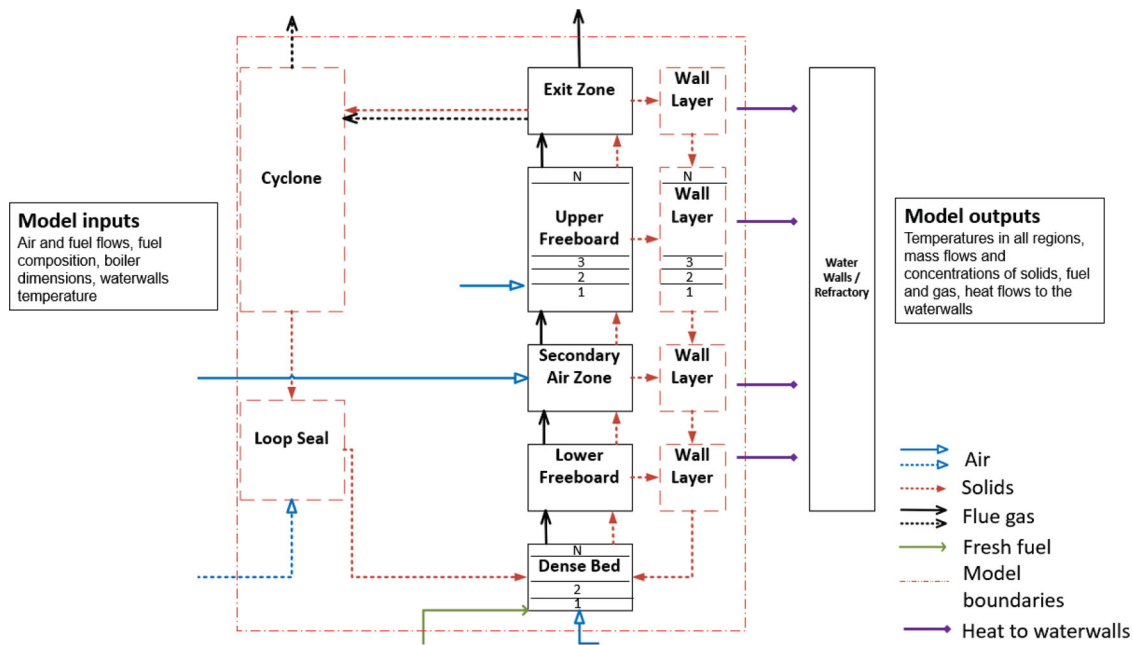
Figure 1. Schematic of the model. The solid-line elements are present in both the BFB and CFB configurations, while the dashed-line elements are only present in the CFB. The figure also shows the waterwalls and refractory as given temperature boundary condition.

specific set of assumptions and mechanisms, ii) utilizing semi-empirical expressions based on a general theoretical ground and derived from data covering a wide range of operating conditions and sizes rather than correlations derived from measurements in singular units, and iii) calibrating and validating the model with site data for both types of units and at various load levels. Figure 1 shows a schematic representation of the main control volumes and their connections. While some of the control volumes are used in both the BFB and CFB modes (solid line in Figure 1), others are exclusive to the CFB mode (dashed-line elements in Figure 1). Similarly, the volumes in the furnace exchange gas flows (black solid arrows) and solid flows in the CFB mode (red dashed arrows).

The control volumes are modeled as continuously stirred tank reactors, i.e., assuming perfect mixing within the volume. Note that the regions that exhibit a plug-flow behavior, e.g., the upper freeboard and the gas flow in the dense bed, are modeled as a consecution of N stirred tank reactors. The dynamic mass and energy balances are formulated in each of them, accounting for the three phases included in the model: bulk solids, fuel, and gas. From these balances, the concentrations of all the species considered and the temperature are solved for each control volume.

Model inputs consist of boiler geometry, fed air and fuel flows, fuel composition, and boundary temperature in the waterwalls. As an output, the model provides, for all the control volumes defined, the temperature, the heat flow transferred to the walls, and the concentrations and mass flows of solids, fuel classes and gas species.

Inert solids, the addition and removal of which have been neglected, are characterized by a single class of the mean particle size. The fuel phase has been modeled as three conversion classes, to account for the differences in density and particle size that arise as conversion evolves. The gas phase accounts for nine species: H_2, O_2, CO, CO_2, H_2, H_2O, NH_3, H_2S and heavy hydrocarbons (tar). Three homogeneous reactions have been included (oxidation of carbon monoxide, hydrogen and tar) along with char oxidation; the kinetics are taken from previous publications [25, 26]. The waterwalls are modeled as boundary conditions with a given constant temperature, T_w, which in this work is assumed to be equal to the waterside temperature. Refractory material can be present in some regions, in which the heat extraction is set to zero. Note that the thermal inertia introduced by the refractory materials is not included in the model since the domain modeled is defined to end at the wall surface (where boundary conditions are given).

The key differences between the BFB and the CFB configurations are the mechanisms for heat transfer to the walls and the solids hydrodynamics, the mathematical description of which is given below. Gas mixing is used as a calibration factor in both model configurations through the tuning of the effective reaction

rate of the homogeneous reactions by applying a height-dependent rate factor to the kinetic rate (see Appendix A for details).

BFB mode

The bulk solids and fuel phases remain in the dense bed region, making radiation the dominant mechanism driving the heat transfer to the furnace walls. Radiative heat flows to and from each surface inside the furnace (namely, the dense bed surface and the furnace sidewalls and roof), as well as from and to each gas volume. Equation (1) shows the heat balance over a certain surface *surf*, considering radiative heat transfer to be dominant, and Eqs. (2) and (3) expand the values of the radiative heat received $q_{in,surf}$ and emitted $q_{emitted,surf}$.

$$q_{net,surf} = \alpha_w q_{in,surf} - q_{emitted,surf} \qquad (1)$$

$$q_{in,surf} = \sum_j \left((\sigma \varepsilon_j T_j^4 + q''_{in,j}(1 - \varepsilon_j)) \cdot A_j F_{j-surf} \prod_j^s (1 - \alpha_{g,j-surf}) \right)$$

$$+ \sum_k (\sigma \varepsilon_{g,k} T_{g,k}^4 A_k F_{k-surf} \prod_k^s (1 - \alpha_{g,k-surf})) \qquad (2)$$

$$q_{emitted,surf} = \sigma \varepsilon_w T_{surf}^4 A_{surf} \qquad (3)$$

The first term in Eq. (2) refers to the total incoming radiation from other surfaces within the furnace (i.e., other waterwalls or the bed surface). Note that this term consists of the emitted and reflected radiation of the surface *j*, multiplied by the view factor between surfaces *j* and *surf* F_{j-surf}, and by $(1-\alpha)$ of all the control volumes that the flux crosses from *j* to *surf*, so as to account for the fraction that is absorbed by the gas. The second term in Eq. (2) represents the gas radiation from the control volume *k* to the surface *surf* (note that the gas absorption on the way from *k* to *surf* has also been included). The view factors between surfaces and volume and surfaces have been computed according to [27].

Regarding the control volumes occupied by gas, a balance similar to that shown in Eq. (1) is applied. The heat flows emitted and received in a certain gas volume *vol* are computed according to Eqs. (4) and (5).

$$q_{in,vol} = \sum_j \sum_i \left(q_{emitted,j} F_{ji} \prod_k^{surf} ((1 - \alpha_{k,ij})) \alpha_{vol} \right)$$

$$+ \sum_k \sum_i \left(\sigma \varepsilon_{vol,k} A_k F_{ki} T_k^4 \prod_h^{surf} ((1 - \alpha_{h,k-surf})) \alpha_{vol} \right) \qquad (4)$$

$$q_{emitted,vol} = \sigma \varepsilon_{vol} T_{vol}^4 A_{vol} \qquad (5)$$

$$\varepsilon_{vol} = 1 - e^{-k_{vol}L} \qquad (6)$$

The first term in Eq. (4) refers to the absorbed radiation from surface to surface, in which the fraction absorbed by other gas volumes has also been taken into account. The second term accounts for the absorbed fraction from all the gas-to-surface radiation crossing the gas volume *g*. Equation (5) shows the emitted radiation of a gas element (which is equal to the sum of all the gas-gas and gas-surface radiation emitted from the volume *g*).

It is known that the freeboard of BFB boilers contains a small fraction of fine solids (the mass of which is neglected in the model), which will increase the radiation absorbed and emitted by the control volume. Thus, since the amount of solids present in the gas at different heights is not known, the effective emissivity of the control volumes in the freeboard of the BFB is handled in the model as a calibration factor (see Appendix A), where the value of k_{vol} in the expression for the Beer-Lambert Law is tuned, see Eq. (6).

CFB mode

As shown in Figure 1, the CFB mode presented in this work has a 1.5D representation of the furnace, i.e., it accounts for the core-annulus structure of the solids flow. The hydrodynamics of the solids have been implemented according to the model presented by Johnsson et al. [28]. The fraction of solids entrained from the dense bed by the gas flow is computed based on the data published by Djerf et al. [29]. Some of these entrained solids are back-mixed through the furnace wall layers, while the remainder reaches the exit region. The net transfer of solids from the core region to the wall layers at different heights is modeled according to experimental data acquired from several industrial units under different operating conditions [28–35]. Finally, at the exit duct, the solids experience a backflow effect, modeled based on previously published data. Figure 2 illustrates a certain control volume in the riser, showing the flows of solids between the core and wall layer. The model ignores the presence of a gas phase in the wall layers. The mean bulk solids size is treated as a calibration factor (see Appendix A).

Equation (7) formulates the expression used to compute the heat transferred to the waterwalls at a certain height, where A is the heat exchange area assigned to the control volume *i*, h_c is the heat transfer coefficient (calculated according to Breitholtz et al. [1]), and ε is the average emissivity of the suspension

and walls. Radiation is accounted for as proposed by Breitholtz et al [1], i.e., a radiation efficiency η_{rad} is included to account for the increase of radiation when the solids concentration at the wall layers decreases [36]. Note that the temperature governing the radiative heat transfer is that at the core, while the wall-layer temperature is used for the convective heat flow.

$$Q_{wall,i} = h_c \cdot A_i \cdot (T_{wl} - T_w) + \eta_{rad} \cdot \varepsilon \cdot A_i \cdot \sigma$$
$$\cdot (T_{core}^4 - T_w^4) \qquad (7)$$

Reference units

Two industrial furnaces with sizes and designs typical of biomass-based FB plants are selected as reference plants. The furnaces are used in [22] for steady-state and transient validation of the model, while in the present work represent the basis for the analysis. Table 1 lists the main design and operational parameters of each unit used as input for the model. Both units work with biomass in the form of wood chips whose specific composition used in each of the reference plants is shown in Table 2.
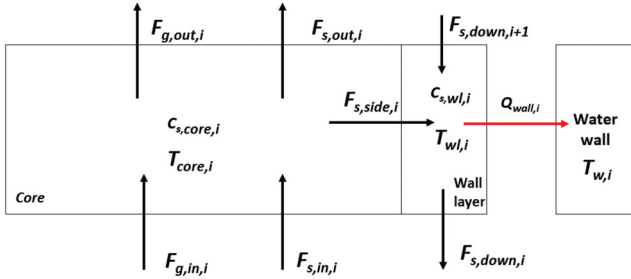

Figure 2. Schematic of the mass flows entering and exiting the control volumes at a certain height of the CFB furnace. The figure shows the concentrations and temperatures calculated in each volume. The waterwall box acts as the temperature boundary condition.

Simulations of transient operation

The model described above is applied to investigate the differences in transient behavior between industrial BFB and CFB boilers. To establish a fair comparison and avoid effects related to the size of the unit, the CFB model is scaled-up to a 130-MW unit. After being validated with operational data from a 100-MW industrial unit [22], the model is parameterized again to resemble a larger unit with similar operational conditions. Thus, the cross-sectional area is increased to maintain constant gas velocity and the height of the furnace is increased to maintain the same concentration of solids at the top of the riser as in the 100-MW reference unit. The superheater inserted in the furnace has its load increased so as to keep the same gas temperature at the furnace exit, while the air-to-fuel ratio and the primary-to-secondary air ratio are kept constant.

Open-loop tests are a well-established method for evaluating the inherent dynamics of a certain system. These tests include the introduction of separate step-changes in process inputs of interest and letting the uncontrolled system evolve toward stabilization. Performing this type of analyses in industrial plants is often complicated as there are operational and safety limitations, what makes dynamic models a great tool for the evaluation of the inherent dynamics of a process. Since the open-loop tests require the system to be substantially perturbated so the dynamics can be clearly measured, the simulated scenarios are a load reduction from 100% to 75% (keeping the air-to-fuel and primary-to-secondary air ratios constant), as well as a fuel moisture content increase of 5% when the units are running at 100% load. The latter is meant to give an example illustrating the response to a change in the heating value of the feedstock (a common situation in e.g., waste combustion) but stands also for a real-life scenario in a specific share of the fluidized bed plants (those devoted to district heating where moist fuel can be used to support the control of the

Table 1. Design and operational parameters of the industrial reference units.

	Reference unit	
Parameter, unit	BFB furnace	CFB furnace
Furnace dimensions, m	$9.18 \times 8.67 \times 30$	$8.5 \times 4.1 \times 21$
Waterwalls area, m^2	885	425
Cyclone volume, m^3	–	77.5×2
Fuel flow, kg/s	13.8	12
Air flow, Nm^3/s	38	30.6
Primary/secondary air ratio	0.74	0.78
Recirculated flue gas flow, Nm^3/s	14	–
Air inlet temperature, °C	260	190
Steam temperature, °C	344	290
Heat extracted by immersed superheaters, MW	18.3	2.5
Bulk solids density, kg/m^3	2600	2655
Solids average size, μm	450	200

Table 2. Proximate and ultimate analyses and heating values of the wood chips used to model the reference units.

Proximate analysis, wt%	BFB furnace	CFB furnace
Moisture	40.00	54.00
Volatiles	47.00	32.00
Char	12.60	13.60
Ash	0.40	0.40
Ultimate analysis (dry, ash-free), wt%		
C		50.60
H		5.90
O		43.20
N		0.08
S		0.04
HHV (dry, ash-free), MJ/kg	17.9	17.0-18.5

furnace-to-convection pass heat extraction ratio and/or the heat-to-power output ratio). The open-loop (uncontrolled) responses of the units are evaluated by applying the changes mentioned above in the form of steps, and then measuring the stabilization times of the main process variables. The stabilization time t_s is computed as the time it takes for a certain process variable to execute 90% of the total change after a certain variation is applied [see Eq. (8), where y_∞ refers to the new steady-state value after the change and Δy is the absolute change in steady-state values before and after the change]. The definition of stabilization time used in this work is in line with the expected noise when measuring temperatures such as the ones the current work deals with. The relative change RC of the variable once the new steady-state is established is computed according to Eq. (9). The process variables selected to perform the comparison are, the temperature in the dense bed, T_{db}; the temperature at the top of the riser before the superheaters, T_{top}; and the heat transferred to the waterwalls, Q_{wall}.

$$y_\infty - 0.1\Delta y < y_\infty < y_\infty + 0.1\Delta y \qquad (8)$$

$$RC = 100 \cdot \frac{y_\infty - y_0}{y_0} \qquad (9)$$

Analysis of the in-furnace characteristic times

In order to assess the influence of the different in-furnace mechanisms on the dynamics of the flue-gas side, a sensitivity analysis is carried out for the load change scenario. For that, three characteristic times representative of each of the three main in-furnace mechanisms are defined:

- Fuel conversion time, τ_{FC} : Among the fuel conversion processes involved, char conversion is assumed to be dominant in front of drying and devolatilization in terms of dynamic response, as it is the slowest of these three while it represents a significant heat release regardless of the fuel type (see [37] for a comprehensive review of fuel conversion mechanisms in biomass-fired FB combustors). Hence, the characteristic time for fuel conversion is defined as shown in Eq. (10). Note that t_{char} is computed according to the shrinking sphere regime (see [22] for details).

$$\tau_{FC} = t_{char} \qquad (10)$$

- Heat transfer time, τ_{HT} : with the gas-solids heat transfer being high in FB units, the dynamics of the heat transfer are governed by the thermal inertia of the furnace inventory. This time is defined as the ratio between the thermal mass of the inventory and the inflow (i.e., involving heat capacity, see Eq. (11)).

$$\tau_{HT} = \frac{\sum m_i C_{p,i}}{\sum F_i C_{p,i}} \qquad (11)$$

- Fluid-dynamics time, τ_{FD} : this time serves to consider the time taken to convey mass and heat after an operational variation. For the CFB mode, the establishment of a new solids flow in the hot loop is considered to be dominant, as it is the slowest of the fluid-dynamics mechanisms with significance (gas residence times are in the order of 5–10 s for industrial scale CFB units [22]). Thus, the fluid-dynamics time is here defined as the time for solids external circulation, i.e., through the cyclone and loop seal (Eq. (12)). In the BFB mode, however, where the solids are assumed to remain in the dense bed and do not yield a significantly different solids flow after operational variation, the fluid dynamics time is taken as the residence time of the gas phase in the furnace (Eq. (13)).

$$\tau_{FD,CFB} = \tau_{riser} + \tau_{cyclone} + \tau_{loop-seal} \qquad (12)$$

$$\tau_{FD,BFB} = \tau_{gas} \qquad (13)$$

Table 3 lists the variables that have been varied in each of the model modes as well as the resulting characteristic times. Note that the characteristic time of the fluid dynamics in the BFB mode cannot be varied without altering the geometry of the furnace, i.e., modifying the height, and is therefore not varied here. In the CFB case, however, the loop seal size is varied in order to alter $\tau_{loop-seal}$ and thus $\tau_{FD,CFB}$ (see Eq. (12)) while keeping the same furnace geometry and solids properties. Note that considering all the possible combinations yields 3×3 cases for BFB and $3 \times 3 \times 3$ for CFB.

Table 3. Variations of the characteristic times of the three in-furnace mechanisms (as defined in Eqs. (10)–(13)) included in the analysis.

| In-furnace mechanism	Variable varied	Varied values	Resulting characteristic times [s]	
			BFB	CFB
Fluid dynamics	Size of loop seal (for CFB)	3.5-8-12 m^3	(10, 10, 10)	(40, 95, 145)
Fuel conversion	Char conversion time	30-10-450 s	(30, 150, 450)	(30, 150, 450)
Heat transfer	Solids heat capacity	800-1150-1500 J/kgK	(450, 650, 850)	(300, 450, 600)
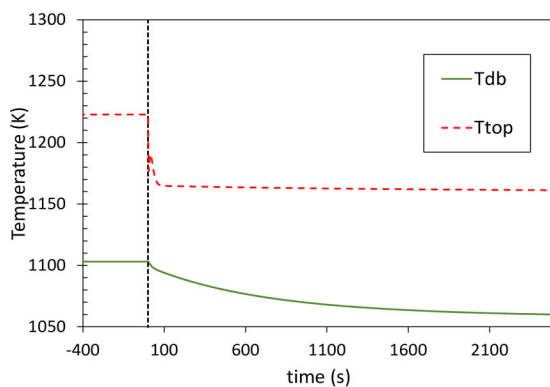
a) Simulated temperatures in dense bed and before superheaters in the BFB
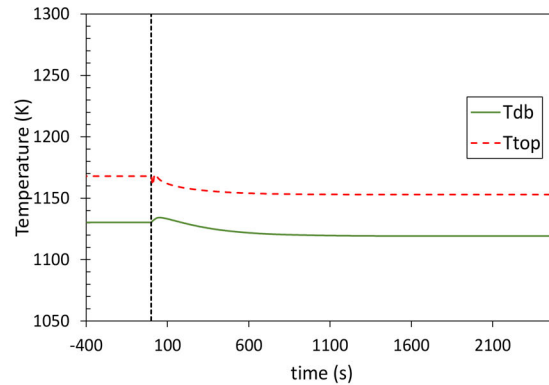
b) Simulated temperatures in dense bed and before cyclone in the CFB
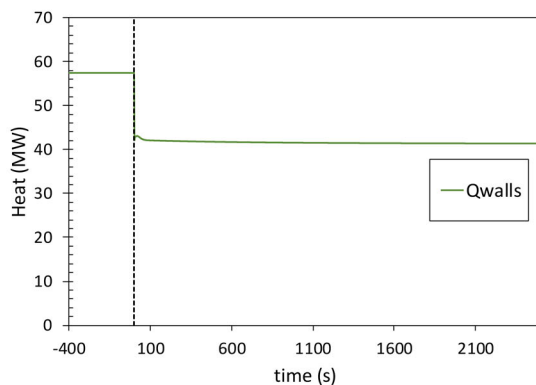
c) Simulated heat transfer to the waterwalls in the BFB
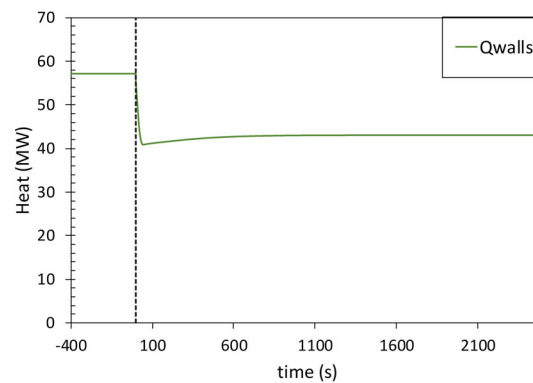
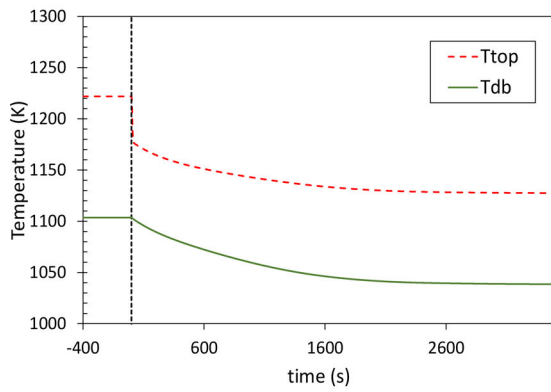d) Simulated heat transfer to the waterwalls in the CFB

Figure 3. Transient responses in the BFB and CFB boilers for the relevant process variables after a 25% load reduction step-change is introduced at $t=0$ (represented with dashed black line).

Results and discussion

Figure 3 shows the responses of the selected process variables resulting from the introduction of a step-down in load at $t=0$ (marked as a dashed line). The corresponding responses of the variables when a step-up in fuel moisture is introduced are plotted in Figure 4. The stabilization times and relative changes in the variables of interest are listed in Table 4.

It is evident from Figure 3b that the temperatures in the CFB unit exhibit an abrupt initial response, both in the dense bed and at the top of the riser, which is a phenomenon that is not observed in the

BFB unit. This indicates that the presence of solids in the freeboard is related to the initial abrupt changes. It is observed in both units a faster response of the temperature in the upper furnace than at the bottom, as well as a larger relative change. This difference in stabilization times becomes even larger in the BFB case, where the top region stabilizes 14-times faster than the bottom region. This observation relates to the differences in heat capacity between regions: the dense bed contains a larger fraction of solids and, therefore, has a higher heat capacity than the top of the freeboard, which makes it less sensitive to changes,
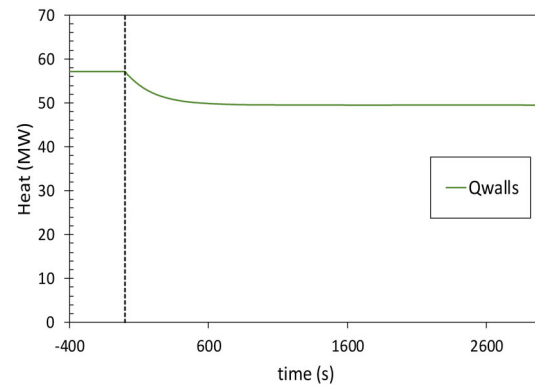
a) Simulated temperatures in dense bed and before superheaters in the BFB
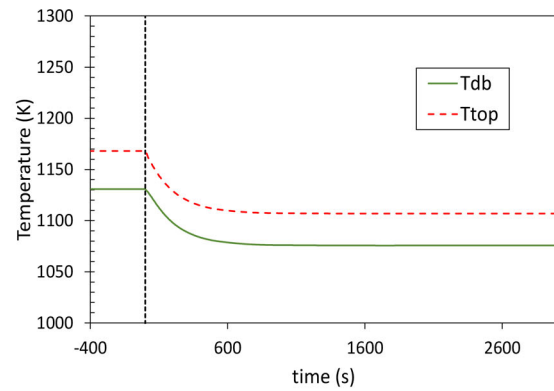
b) Simulated temperatures in dense bed and before cyclone in the CFB
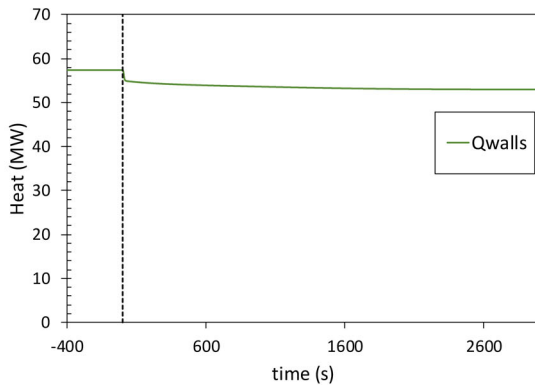
c) Simulated heat transfer to the waterwalls in the BFB

d) Simulated heat transfer to the waterwalls in the CFB

Figure 4. Transient responses in the BFB and CFB boilers for the relevant process variables after a 5% step-increase in fuel moisture is introduced at $t = 0$ (represented with dashed black line).

Table 4. Stabilization times (t_s) and relative changes (RC) in the relevant process variables when a 25% step-down in load and a 5% step-up in fuel moisture are introduced, respectively.

	BFB			CFB		
Load reduction	T_{db}	T_{top}	Q_{wall}	T_{db}	T_{top}	Q_{wall}
t_s (s)	925	67	45	860	520	310
RC (%)	4.1	4.87	27.1	1.2	1.6	24.8
Moisture increase						
t_s (s)	1680	560	1170	470	450	210
RC (%)	5.8	7.1	7.8	4.9	5.0	13.4

although it takes more time to achieve stabilization. As shown in Figure 3c, the heat transferred to the waterwalls decreases sharply in the BFB boiler, reaching stabilization in less than 1 minute (45 s; see Table 4). In contrast, the CFB boiler shows a sudden drop in transferred heat followed by a slight increase toward stabilization, which is reached after 310 s. The detected discrepancy between the units is attributed to the fact that the BFB unit is radiation-driven whereas the CFB unit is largely affected by the convection of solids.

When a 5% step-up in fuel moisture content is simulated, the temperatures simulated in both the CFB and BFB units fall smoothly toward a lower steady-state value, as seen in Figure 4a,b. In both boilers, the dense bed exhibits a slower response than the top of the riser, as most of the fuel drying (all of it in the BFB unit) occurs in the dense bed, a region that is characterized by the presence of a large mass of solids. Note that the stronger impact on the heat transfer to waterwalls observed for the CFB boiler in Table 4 reflects the fact that the CFB unit is modeled with a fuel that has a higher moisture content than that in the BFB unit (see Table 2). It is also shown in Table 4 that the relative changes in the BFB temperatures differ significantly between the bottom and top of the boiler, linked to the assumption that all the solids remain in the bed. This difference becomes less pronounced in the CFB unit, where the solids are circulating and, therefore, the impact of increased drying is evenly distributed across the furnace. Another aspect
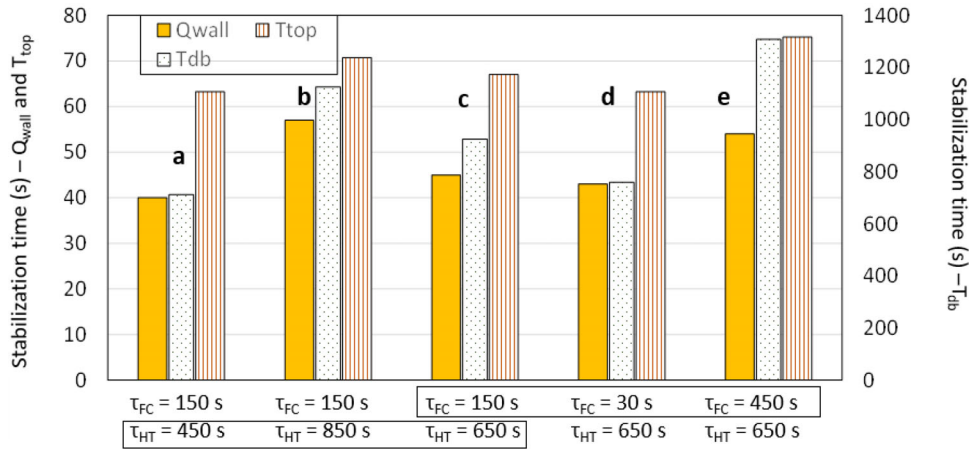
Figure 5. Stabilization times of the main in-furnace variables in the BFB unit under different variations of characteristic times for the three in-furnace mechanisms (FC: fuel conversion, HT: heat transfer). Note that the characteristic time of the fluid dynamics has not been varied (see Table 3).

Table 5. Simplified expressions for the dependency of the stabilization times (t_s) of the main process variables on the characteristic times of the three in-furnace mechanisms (FD: fluid dynamics, FC: fuel conversion, HT: heat transfer).

Unit	Variable	Expression	
BFB	T_{db}	$t_{s,db} \approx \tau_{FC} + \tau_{HT}$	(14)
	T_{top}	$t_{s,top} \approx \tau_{FD} + 0.05\, t_{s,db}$	(15)
	Q_{wall}	$t_{s,Q} \approx t_{s,top}$	(16)
CFB	T_{db}	$t_{s,db} \approx \tau_{FC} + \tau_{HT} + \tau_{FD}$	(17)
	T_{top}	$t_{s,top} \approx 0.7\, t_{s,db}$	(18)
	Q_{wall}	$t_{s,Q} \approx 0.9\tau_{FC} + 0.2\,\tau_{FD} + 0.4\,\tau_{HT}$	(19)

that can be extracted from Figure 4 is the fact that the abrupt change in the CFB temperature observed for a load change disappears when it comes to a change in moisture content in relation with what was stated above: the change in solids fluxes (which is dependent upon the gas velocity) is responsible for the initial abrupt changes observed in the upper part of the furnace.

In summary, it can be stated that the CFB unit, as compared to the BFB, is less sensitive to changes in load and fuel, while presenting a slower response to such changes. This aspect is directly related to the heat capacity (i.e., mass of solids) within the boiler, an aspect that gains importance within each unit: furnace regions with a large heat capacity, such as the dense bed, react more slowly to changes, with changes in the steady-state values being less-severe than those seen in regions with lower levels of solids, i.e., at the top of the furnace.

When the characteristic times of the in-furnace mechanisms are varied according to the values presented in Table 3, new open-loop stabilization times for the −25% load change are obtained and, for a selection of 5 illustrative BFB cases, plotted in Figure 5 (note the double y-axis). Table 5 formulates simplified expressions (Eqs. (14)–(19)) that roughly relate the in-furnace stabilization times to the characteristic

times of the mechanisms investigated, according to the discussion below. Note that the selection of a different stabilization time for computation of the furnace dynamics would not alter the trends shown in Table 5 but the coefficients in the expressions.

First, the temperature in the dense bed, T_{db} exhibits much longer stabilization times (600–1500 s for all the cases investigated) than the temperature at the furnace top, T_{top} and the heat extracted from the furnace walls, Q_{wall}. This is mainly due to the fact that the dense bed in BFB units houses both the solids and fuel inventory and thus the fuel conversion and the main share of the furnace thermal inertia. In line with this, the stabilization times of the dense bed temperature correspond roughly to the sum of the characteristic times of these two mechanisms present in the dense bed, i.e., fuel conversion and heat transfer (see Eq. (14) in Table 5). Note that this is a simplification since some other minor mechanisms are also influencing the resulting stabilization time, such as the recirculation of flue gas, or the characteristic times for drying, devolatilization or gas mixing and combustion. The temperature at the top of the furnace and heat transfer to the waterwalls stabilize much faster (60–80 s and 40–70 s, respectively) than that of the bottom dense bed. This is a consequence of the heat transfer to the walls being driven by the change in effective gas emissivity forced by the varied presence of solids fines entrained by the gas, rather than the varying bottom gas temperature. Given the very low thermal inertia of the BFB furnace top, its temperature can then be expressed as a function of the residence time of the gas conveying the change in effective gas emissivity (which in the investigated unit has a value of 10 s as shown in Table 3) and, to a
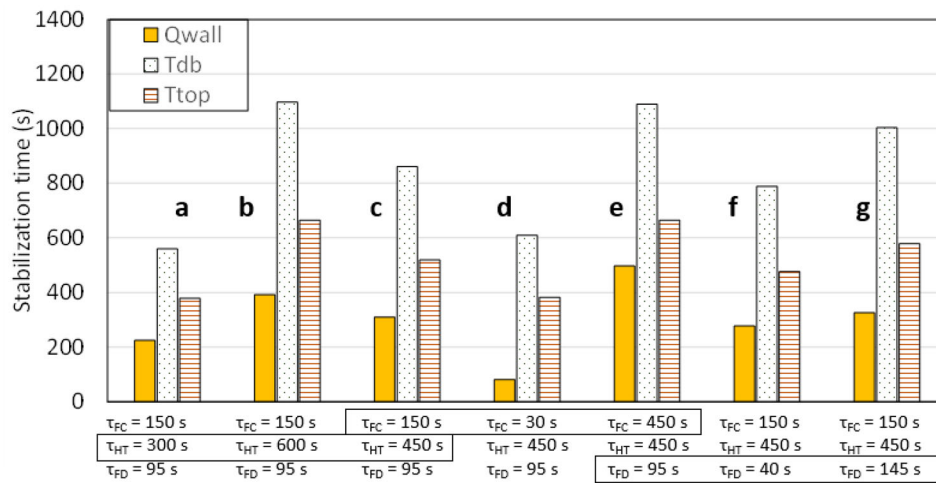
Figure 6. Stabilization times of the main in-furnace variables in the CFB unit under different variations of characteristic times for the three in-furnace mechanisms (FD: fluid dynamics, FC: fuel conversion, HT: heat transfer).

minor extent (note the low coefficient in Eq. (15) in Table 5), the stabilization time for the temperature of the gas leaving the bottom region. With the heat transfer to the waterwalls being dependent on the gas temperature and effective emissivity, its characteristic time is found roughly equal to that for the temperature at the furnace top (which already accounts for the time to establish the new gas emissivity), see Eq. (16) in Table 5.

Stabilization times for the CFB cases show different dependencies than those observed for BFB conditions and are illustrated in Figure 6 by a selection of 7 cases. Firstly, a more uniform distribution of the stabilization times for the CFB cases in comparison to BFB conditions can be observed, with temperatures stabilizing in times of the same order of magnitude. This can be explained by the increased mass and thermal mixing in CFB units. Regarding the stabilization time of furnace temperatures, a relatively uniform effect of the three mechanisms considered for CFB conditions (fluid-dynamics, fuel conversion, heat transfer) is observed and in the bottom region it can be directly approximated as the sum of the three characteristic times (Eq. (17) in Table 5). Thus, the thermal stabilization of the dense bed can be interpreted as a chain consisting of, first, the stabilization of the heat released by fuel conversion, after which the thermal inertia of the furnace inventory (mostly concentrated in the dense bed) needs to stabilize along its thermal time, after which the circulating solids need the characteristic fluid-dynamical time to thermally stabilize the whole hot loop feeding back material into the dense bed. These processes are obviously overlapping, but stabilization is governed by the finalization (i.e., the tail) of each of them and the pass-on of this tail to the next phenomenon in the chain; thereby final stabilization is better approached by the sum of

characteristic times rather than by selecting the maximum of the three. As for the upper furnace temperature, stabilization generally occurs roughly 30% faster than that at the furnace bottom (Eq. (18) in Table 5). Finally, the dynamics of the heat transfer to the walls (Eq. (19) in Table 5) are sensitive to all of the variations simulated and mostly influenced by the fuel conversion time (see cases c and d in Figure 6), while is quite insensitive to the fluid dynamics (see cases f and g in Figure 6).

Conclusions

A dynamic model of the flue gas sides of large-scale bubbling and circulating fluidized bed boilers previously published by the authors is here used to simulate two industrial units in transient operation. A brief description of the model with a special focus on the differences between the bubbling and circulating modes is included. The model is thereafter applied to compare the transient behaviors of a BFB combustor and a CFB combustor of the same size (130 MWth). For this purpose, two different transient scenarios are investigated. A 25% step-down in load and a 5% step-up in fuel moisture are simulated, while the system is maintained in open-loop (uncontrolled) and the evolution with time of the main process variables is analyzed. Furthermore, this work includes an in-depth analysis and comparison of the mechanisms driving the in-furnace dynamics.

The results obtained from the open-loop test show that:

- Heat transfer to the waterwalls stabilizes faster in the BFB unit when the load is decreased.
- The temperatures in the CFB boiler are less affected by changes than those in the BFB boiler,

which is attributed to the larger thermal inertia inherent to the solids fluxes in the circulating system. The presence of solids along the furnace causes the temperatures in the CFB to exhibit an abrupt initial response when a step in the air velocity is introduced, which is something that does not occur in the BFB because the presence of solids therein is limited to the dense bottom bed.

- Large differences in temperature are observed between the bottom and top regions of the furnace due to the differences in heat capacity caused by the inventory of solids. This difference is most-pronounced in the BFB case, which means that the top region stabilizes up to 10–15-times faster than the bottom region.
- The CFB unit is better than the BFB unit at dealing with changes in fuel moisture content, as its response is faster and more evenly distributed throughout the furnace.

Exploring the stabilization times of the flue gas side of FB combustors through varied characteristic times for the fluid-dynamics, fuel conversion and heat transfer shows the following:

- For BFB units, the stabilization time of the heat transfer to the walls is mostly driven by the gas residence time which governs the change in effective emissivity of the fines-containing gas. However, the temperature in the bottom part of the furnace is largely affected by the characteristic time of the fuel conversion and heat transfer (thermal inertia).
- In CFB furnaces the stabilization time of the heat transfer to the walls is largely affected by the characteristic times of the fuel conversion and the heat transfer.

These results have been converted into simple mathematical expressions that can be of interest when assessing the expected dynamics of a certain unit based on its in-furnace characteristic times. The results presented in this work provide tools to assess the transient capabilities of a given furnace with a certain size, fuel, and bulk solids. Furthermore, the findings of this work are relevant to fluidized bed manufacturers and operators in terms of the design and choice-making of units for the more flexible operation envisioned in future energy systems with an increased share of non-dispatchable energy.

Acknowledgments

Disclosure statement

The authors declare no competing financial interest.

Notes on contributors

Guillermo Martinez Castilla is a Ph.D. student at the Division of Energy Technology of Chalmers University of Technology, Sweden. He holds a Double Master of Science degree in Energy Engineering at University of Iceland and Chalmers University in Sweden. His current work focuses on the development of dynamic models at both reactor and process levels of novel energy processes involving large-scale fluidized bed reactors.

Rubén M. Montañés is a Research Scientist at SINTEF Energy Research in Norway. He received a Double Master of Science Degree consisting of a M.Sc. in Mechanical Engineering from the Faculty of Engineering at Lund University in Sweden and a M.Sc. in Industrial Engineering from the Polytechnic University of Valencia in Spain. He holds a Ph.D. in Energy and Process Engineering from the Norwegian University of Science and Technology in Trondheim, Norway, and conducted post-doctoral studies at Chalmers University of Technology in Sweden. His research interests include thermal process design optimization, dynamic process modeling and simulation, process control, operational flexibility of low carbon thermal power plants and CO2 capture.

David Pallarès is a Professor at Chalmers University of Technology, Sweden. He focuses his research in fluidization and aims at developing knowledge and tools for the design, scale-up and performance of established and novel fluidized-bed processes. His work pays special attention to the use of non-fossil fuels such as biomass and renewable waste.

Filip Johnson is a Professor at Chalmers University of Technology, Sweden. His research focuses on measures to reduce the climate impact of the energy system. The research deals partly with technical issues concerning electricity and heat production and partly with how the entire energy system can be adjusted to the year 2050. The latter is based on technical-economic studies

regarding how climate impact from the energy system can be reduced in a cost-effective way.

References

[1] C. Breitholtz, B. Leckner, and A. P. Baskakov, "Wall average heat transfer in CFB boilers," *Powder Technol.*, vol. 120, no. 1-2, pp. 41–48, 2001. DOI: 10.1016/S0032-5910(01)00345-X.

[2] J. Koornneef, M. Junginger, and A. Faaij, "Development of fluidized bed combustion — an overview of trends, performance and cost," *Prog. Energy Combust. Sci.*, vol. 33, no. 1, pp. 19–55, 2007. DOI: 10.1016/j.pecs.2006.07.001.

[3] J. DeFusco, P. McKenzie, and W. Stirgwolt, "A comparison of fluid-bed technologies for renewable energy applications," paper presented at the Renewable Energy World Conference, Austin, Texas, Feb. 23–25, 2010.

[4] R. M. Montañés, J. Windahl, J. Pålsson, and M. Thern, "Dynamic modeling of a parabolic trough solar thermal power plant with thermal storage using modelica," *Heat Transf. Eng.*, vol. 39, no. 3, pp. 277–292, 2018. DOI: 10.1080/01457632.2017.1295742.

[5] X. He, Y. Wang, D. Bhattacharyya, F. V. Lima, and R. Turton, "Dynamic modeling and advanced control of post-combustion CO_2 capture plants," *Chem. Eng. Res. Des.*, vol. 131, pp. 430–439, 2018. DOI: 10.1016/j.cherd.2017.12.020.

[6] A. Cammi, F. Casella, M. E. Ricotti, and F. Schiavo, "An object-oriented approach to simulation of IRIS dynamic response," *Prog. Nucl. Energy*, vol. 53, no. 1, pp. 48–58, 2011. DOI: 10.1016/j.pnucene.2010.09.004.

[7] E. Martelli, F. Alobaid, and C. Elsido, "Design optimization and dynamic simulation of steam cycle power plants: a review," *Front. Energy Res.*, vol. 9, pp. 1–31, Jul. 2021. DOI: 10.3389/fenrg.2021.676969.

[8] J. Saastamoinen, "Modelling of dynamics of combustion of biomass in fluidized beds," *Therm. Sci.*, vol. 8, no. 2, pp. 107–126, 2004. DOI: 10.2298/TSCI0402107S.

[9] J. Sandberg, R. B. Fdhila, E. Dahlquist, and A. Avelin, "Dynamic simulation of fouling in a circulating fluidized biomass-fired boiler," *Appl. Energy*, vol. 88, no. 5, pp. 1813–1824, 2011. DOI: 10.1016/j.apenergy.2010.12.006.

[10] M. Zlatkovikj, V. Zaccaria, I. Aslanidou, and K. Kyprianidis, "Simulation study for comparison of control structures for BFB biomass boiler," paper presented at the 61st SIMS Conference on Simulation and Modelling, Oulu, Finland, Sept. 2020, pp. 107–115.

[11] S. Suojanen, E. Hakkarainen, M. Tähtinen, and T. Sihvonen, "Modeling and analysis of process configurations for hybrid concentrated solar power and conventional steam power plants," *Energy Convers. Manag.*, vol. 134, pp. 327–339, 2017. DOI: 10.1016/j.enconman.2016.12.029.

[12] C. K. Park and P. Basu, "A model for prediction of transient response to the change of fuel feed rate to

[13] a circulating fluidized bed boiler furnace," *Chem. Eng. Sci.*, vol. 52, no. 20, pp. 3499–3509, 1997. DOI: 10.1016/S0009-2509(97)00128-0.

Y. Chen and G. Xiaolong, "Dynamic modeling and simulation of a 410 t/h Pyroflow CFB boiler," *Comput. Chem. Eng.*, vol. 31, no. 1, pp. 21–31, 2006. DOI: 10.1016/j.compchemeng.2006.04.006.

[14] S. Kim, S. Choi, J. Lappalainen, and T. H. Song, "Dynamic simulation of the circulating fluidized bed loop performance under the various operating conditions," *Proc. Inst. Mech. Eng. Part A J. Power Energy*, vol. 233, no. 7, pp. 901–913, 2019. DOI: 10.1177/0957650919838111.

[15] D. Stefanitsis, A. Nesiadis, and K. Koutita, "Simulation of a CFB boiler integrated with a thermal energy storage system during transient operation," Frontiers in Energy Research, Vol. 8, Article no. 169 (14 pages), pp. 1–14, Sept. 2020. DOI: 10.3389/fenrg.2020.00169.

[16] N. Zimmerman, K. Kyprianidis, and C.-F. Lindberg, "Waste fuel combustion: dynamic modeling and control," *Processes*, vol. 6, no. 11, pp. 222, 2018. DOI: 10.3390/pr6110222.

[17] J. Findejs, V. Havlena, J. Jech, and D. Pachner, "Model based control of the circulating fluidized bed boiler," *IFAC Proc.*, vol. 42, no. 9, pp. 44–49, 2009. DOI: 10.3182/20090705-4-SF-2005.00010.

[18] T. Kataja and Y. Majanne, "Dynamic model of a bubbling fluidized bed boiler," paper presented at the 14th Nordic Process Control Workshop, Espoo, Finland, Aug. 23–25, 2007, pp. 140–149.

[19] N. Selçuk and E. Degirmenci, "Dynamic simulation of fluidized bed combustors and its validation against measurements dynamic simulation of fluidized bed combustors and its validation against measurements," *Combust. Sci. Technol.*, vol. 167, no. 1, pp. 1–27, Dec. 2001. DOI: 10.1080/00102200108952175.

[20] A. Galgano, P. Salatino, S. Crescitelli, F. Scala, and P. L. Maffettone, "A model of the dynamics of a fluidized bed combustor burning biomass," *Combust. Flame*, vol. 140, no. 4, pp. 371–384, 2005. DOI: 10.1016/j.combustflame.2004.12.006.

[21] V. K. Surasani, F. Kretschmer, P. Heidecke, M. Peglow, and E. Tsotsas, "Biomass combustion in a fluidized-bed system: an integrated model for dynamic plant simulations," *Ind. Eng. Chem. Res.*, vol. 50, no. 17, pp. 9936–9943, 2011. DOI: 10.1021/ie200537m.

[22] G. Martinez Castilla, R. M. Montañés, D. Pallares, and F. Johnsson, "Dynamic modeling of the reactive side in large-scale fluidized bed boilers," *Ind. Eng. Chem. Res.*, vol. 60, no. 10, pp. 3936–3956, 2021. DOI: 10.1021/acs.iecr.0c06278.

[23] Modelica Association, "Modelica and the Modelica Association," 1996. [Online]. Available: https://www.modelica.org/. Accessed: May 14, 2021.

[24] D. Systemes, "Dymola systems engineering," 2021. [Online]. Available: https://www.3ds.com/products-services/catia/products/dymola/. Accessed: Jun 15, 2021.

[25] R. C. Flagan and J. H. Seinfeld, *Fundamentals of Air Pollution Engineering*. Englewood Cliffs, NJ: Prentice Hall, 1988.

[26] F. L. Dryer and C. K. Westbrook, "Simplified reaction mechanisms for the oxidation of hydrocarbon fuels in flames," *Combust. Sci. Technol.*, vol. 27, no. 1-2, pp. 31–43, 1981. DOI: 10.1080/00102208108946970.

[27] F. P. Incropera, D. P. DeWitt, T. L. Bergman, and A. S. Lavine, *Fundamentals of Heat and Mass Transfer*, 6th ed. Hoboken, NJ: Wiley, 2007.

[28] F. Johnsson, W. Zhang, and B. Leckner, "Characteristics of the formation of particle wall layers in CFB boilers," paper presented at the 2nd Int. Conf. on Multiphase Flow, Kyoto, Japan, April 37, 1995, vol. 3, pp. 25–32.

[29] T. Djerf, D. Pallarès, and F. Johnsson, "Solids flow patterns in large-scale circulating fluidised bed boilers: experimental evaluation under fluid-dynamically down-scaled conditions," *Chem. Eng. Sci.*, vol. 231, pp. 116309, Dec. 2021. DOI: 10.1016/j.ces.2020.116309.

[30] H. Yang, G. Yue, X. Xiao, J. Lu. and Q. Liu, "1D modeling on the material balance in CFB boiler," *Chem. Eng. Sci.*, vol. 60, no. 20, pp. 5603–5611, 2005. DOI: 10.1016/j.ces.2005.04.081.

[31] F. Johnsson and B. Leckner, "Vertical distribution of solids in a CFB-furnace," paper presented at the *13th International conference on fluidized-bed combustion*, Orlando, FL, May 7–10, 1995, pp. 719–725.

[32] T. Djerf, "Solids flows in circulating fluidized beds: explorations of phenomena with applications to boilers," Licentiate Dissertation, Dept. Space, Earth and Environment, Division of Energy Technology, Chalmers University of Technology, Gothenburg, Sweden, 2020.

[33] H. I. Mathekga, B. O. Oboirien and B. C. North, "A review of oxy-fuel combustion in fluidized bed reactors," *Int. J. Energy Res.*, vol. 40, no. 7, pp. 878–902, Jan. 2016. DOI: 10.1002/er.3486.

[34] L. Lafanechere and L. Jestin, "Study of a circulating fluidized bed furnace behavior in order to scale it up to 600 MWe," paper presented at the 13th International Conference on Fluidized-Bed Combustion, Orlando, FL, May 7–10, 1995, pp. 971–976.

[35] P. Mirek, "Influence of the model scale on hydrodynamic scaling in CFB boilers," *Braz. J. Chem. Eng*, vol. 33, no. 4, pp. 885–896, 2016. DOI: 10.1590/0104-6632.20160334s20150348.

[36] K. Everaert, J. Baeyens, and K. Smolders, "Heat transfer from a single tube to the flowing gas-solid suspension in a CFB riser," *Heat Transf. Eng.*, vol. 27, no. 6, pp. 66–70, 2006. DOI: 10.1080/01457630600674741.

[37] K. Y. Kwong and E. J. Marek, "Combustion of biomass in fluidized beds: a review of key phenomena and future perspectives," *Energy Fuels*, vol. 35, no. 20, pp. 16303–16334, 2021. DOI: 10.1021/acs.energy-fuels.1c01947.

Appendix A: Model calibration factors

The value of the calibration factors after tuning the model to resemble the reference units are shown in Table A1. Note that the value of the effective reaction rate is varied across the furnace height while the values of the solids particle size and the volumetric absorptivity are left constant with height. Nonetheless, the value of the absorptivity is changed with load. See [22] for details on the determination and use of these calibration factors.

Table A1. Calibration factors after model calibration to resemble the reference units. See [22] for details.

Calibration factor	Rate factor	Average solids particle size	Volumetric absorptivity
BFB mode	$[10^{-5}, 10^1]$		$[0.5, 8] *10^{-3}$ 1/m
CFB mode	$[10^{-5}, 10^1]$	350 μm	